Dalton Transactions

Accepted Manuscript

This article can be cited before page numbers have been issued, to do this please use: T. Torres, M. Sánchez Carballo, M. Urbani, A. K. Chandiran, D. Gonzalez-Rodriguez, P. Vazquez, M. Grätzel and N. Mohammad K., *Dalton Trans.*, 2014, DOI: 10.1039/C4DT01357C.

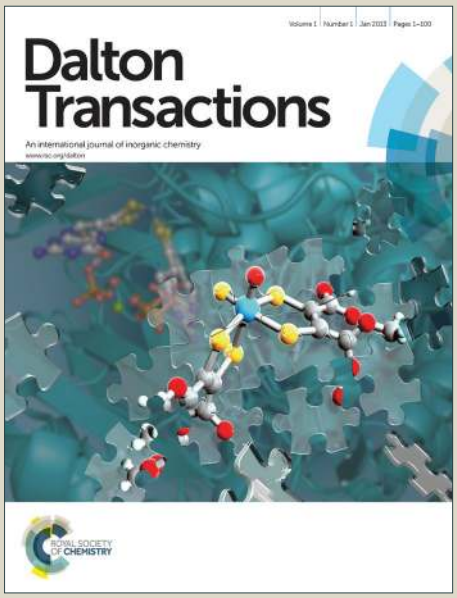

ROYAL SOCIETY OF CHEMISTRY

www.rsc.org/dalton

View Article Online
DOI: 10.1039/C4DT01357C

Dalton Transactions

RSCPublishing

ARTICLE

Branched and bulky substituted Ruthenium sensitizers for Dye-Sensitized Solar Cells

Cite this: DOI: 10.1039/x0xx00000x

M. Sánchez Carballo,[a] M. Urbani,[a,b] A. Kumar Chandiran,[c] D. González-Rodríguez,[a] P. Vázquez,[a] M. Grätzel,[c] M.K. Nazeeruddin*[c] and T. Torres*[a,b]

Received 00thxxxxxxxxx 2014,
Accepted 00thxxxxxxxxx 2014

DOI: 10.1039/x0xx00000x

www.rsc.org/

We report on the synthesis, and photovoltaic performances of four novel Ru(II)-bipyridine heteroleptic complexes **TT206-209**, incorporating branched and bulkier alkyl chains compared to their linear analogues **C106** and **CYC-B11** previously reported. In both series, we found that dyes containing 2-methyl-hex-2-yl substitution gave better performances than 1,1-dipropylbutyl. The best overall performances over the four dyes were obtained for **TT207** (**CYC-B11** analogue) that contain 2-methylhex-2-yl type substitution, achieving an overall PCE of 8.5%. Further optimization of **TT207**/DSSCs, with respect to the dye-uptake solvent and electrolyte composition, led to a maximum PCE of 9.1% under AM1.5G standard conditions.

1. Introduction

Until recently, sensitizers based on Ru(II) polypyridyl complexes, such as **N3** or **N719**, had maintained a clear leadership in DSSC since 1993 in terms of solar-to-electric conversion efficiency (PCE), with validated PCE over 11% under AM1.5G standard conditions.[1] Some ruthenium-free sensitizers based on Zn(II)-porphyrin have equalled these performances between 2010-2011,[2,3] and even surpass them recently with PCE over 13%.[4,5] Nonetheless, these kinds of sensitizers stay still the focus of intense studies and efficient sensitizers in DSSCs,[6,7] although environmental and economic considerations due to ruthenium metal, undoubtedly stand out as the most important issue for their possible use in commercial modules. Some of their inherent advantages[6] are their high quantum yield of electron–injection from the MLCT excited state of the dye into the TiO_2 conduction band (CB), slow back electron transfer (BET), wide absorption in the visible region of the solar spectrum up to 700–800 nm, adequate location of their HOMO-LUMO levels with respect to the TiO_2-CB and the redox shuttle in the electrolyte, long-lived excited states, and excellent photochemical stability. Two main important factors have limited further improvements of the performances of these kinds of sensitizers in DSSC: 1) dye–aggregation issues and 2) rather low molar extinction coefficient of absorption. A common strategy to improve the performances of Ru(II)-sensitizers consists of using heteroleptic complex modified analogues of **N3** or **N719**, which incorporate in their molecular structure one ancillary group beneficial to the dye, and maintain one 4,4'-dicarboxylic 2,2-bipyrridine, acting as anchoring group that is needed to attach efficiently the dye on the metal oxide surface.[8,9] Incorporation of alkyl chains in the ancillary group, for instance nonyl chains (n-C_9H_{18}) in **Z907** dye, or bulky hydrophobic groups,[10,11] has proved to be an efficient strategy to improve the performances of a DSSC cell in comparison with the **N3** analogue. These amphiphilic heteroleptic analogues display several advantages compared to the **N3** complex[12]: 1) they help to reduce dye-aggregation, 2) the hydrophobic groups avoid intrusion of water in the operating device, which improve significantly the long-term durability of the device, 3) they enhance the binding strength of the complex onto the TiO_2 surface, 4) the decreased charge on the sensitizer attenuates the electrostatic repulsion which can result in higher dye-loading, and 5) these complexes usually display lower oxidation potential compared to that of the **N3** sensitizer, which increases the reversibility of the Ru(III/II) couple,[13] and hence also enhances the stability of the dye. On the other hand, incorporation of electron-rich π- systems at one bipyridine moiety (most usually at the ancillary group),[8] such as (poly)thiophene,[14-17] furanyl,[18] 3,4-ethylenedioxythiophene (EDOT),[19,20] styryl,[21-24] (oligo)phenylenevinylene,[25] carbazole,[26] or (vinyl)triphenylamine,[27-29] help the Ru(II)-dye to span sunlight over a wider range and with stronger absorption. In parallel, recent efforts have been also devoted to develop alternative thiocyanate-free ruthenium(II) sensitizers to improve long term stability of DSSCs (in few cases, accompanied with improved photovoltaic performances), because the monodentate thiocyanate ligands are believed to be the weakest parts of $RuLL'(NCS)_2$-type complexes.[30-32]

In our previous work,[33] we demonstrated that incorporation of bulky groups in the molecular structure of a Ru(II) dye can

[a]Universidad Autónoma de Madrid, Departamento de Química Orgánica, Cantoblanco, 28049 Madrid, Spain.
[b]Instituto Madrileño de Estudios Avanzados (IMDEA)-Nanociencia, c/ Faraday, 9, Cantoblanco, 28049 Madrid Spain.
[c]Laboratory of Photonics and Interfaces, Institute of Chemical Sciences and Engineering, Swiss Federal Institute of Technology (EPFL), Station 6, CH 1015 – Lausanne, Switzerland.

†Electronic Supplementary Information (ESI) available: Copy of UV, MS, HRMS, ^1H and ^{13}C NMR spectra. See DOI: 10.1039/b000000x/

View Article Online
DOI: 10.1039/C4DT01537C

prevent aggregation resulting in high photocurrents even in the absence of chenodeoxycholic acid, but can lead to lower cell voltages due possible inefficient dye packing. Moreover, it is also known that bulky groups can help to reduce recombination rate between injected TiO_2 electrons and the redox shuttle present in the electrolyte, by forming a blocking layer between them.[34] In this work, we report on the synthesis of four new heteroleptic complexes analogues of **C106**[35] or **CYC-B11**,[36] the dyes **TT206-209** (Chart 1) that contain branched and bulky substitutions. These sensitizers have been tested in TiO_2-DSSC, and their photovoltaic performances compared in each series.

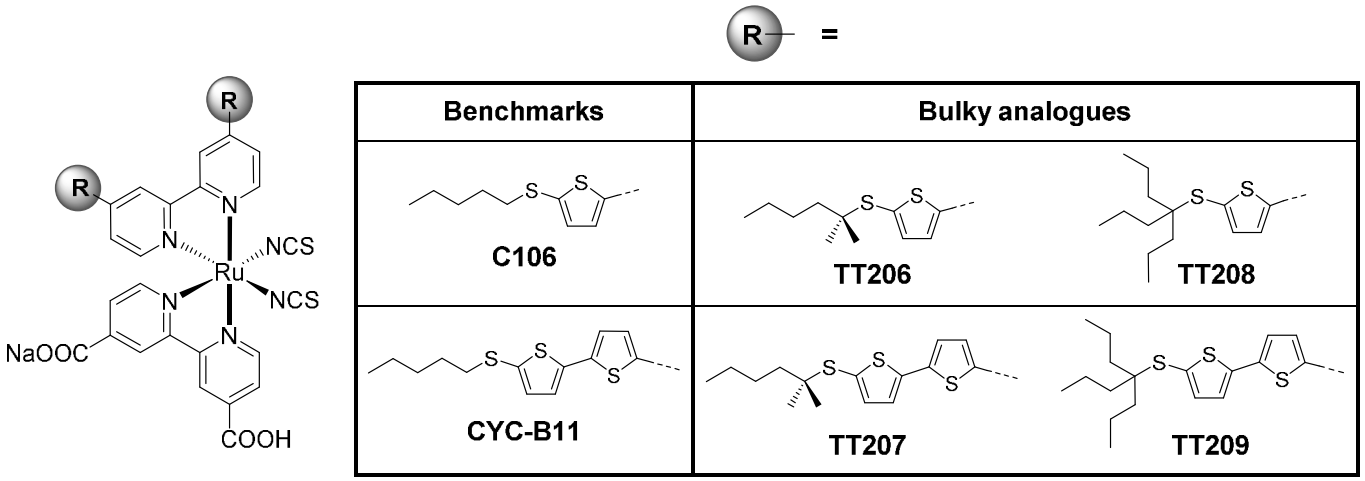

Chart 1 Molecular structures of new ruthenium dyes TT206-209 studied in this work, and previously reported benchmarks C106 and CYC-B11.

2. Experimental section

(a) Materials

Synthetic procedures were carried out under an inert argon atmosphere, in dry solvents unless otherwise noted. All dry solvents (anhydrous grade) were purchased at SDS, used without purification, dried over molecular sieves (3Å), and flushed under argon atmosphere, prior to use. THF was freshly distilled from sodium benzophenoneketyl prior to use. All reagents were reagent grade and used as received without further purification unless otherwise specified. (2,2'-bipyridine)-4,4'-dicarboxylic acid (dcapy), dichloro(*p*-cymene)-ruthenium(II) dimer ($[Ru(p\text{-cymene})Cl_2]_2$) were purchased at TCI, and ammonium thiocyanate(NH_4NCS) at Aldrich. Chromatographic purifications were performed using silica gel 60 SDS (particle size 0.040-0.063 mm) or GE Healthcare Sephadex® LH-20. Analytical thin-layer chromatography was performed using Merck TLC silica gel 60 F254. MS experiments were performed by the *Servicio Interdepartamental de Investigación* (SIdI) at the Autonoma University of Madrid. FAB (matrix: *m*-NBA) and EI-TOF MS/HRMS spectra were recorded on a VG AutoSpec instrument. MALDI-TOF MS/HRMS spectra (matrix: dithranol) were recorded on a Bruker Reflex III spectrometer with a laser beam operating at 337 nm. Poly(ethyleneglycol)-1000 (PEGH) was used as an internal calibration reference for HRMS MALDI-TOF spectra. ^1H (300 MHz) and ^{13}C NMR (75 MHz) spectra were recorded on a Bruker AC-300 equipment; chemical shifts(δ) are given in ppm relative to the residual solvent peak of the deuterated solvent, and coupling constants (*J*) are given in Hz. UV-Vis spectra were recorded on a JASCO V-660 instrument.

(b) Synthesis

Characterisation and detailed synthetic procedures for compounds **1–8** are provided in the Supporting Information.

General procedure for the synthesis of heteroleptic complexes TT206–209

In a sealed tube-flask (closed vessel), a stirred solution of $[Ru(p\text{-cymene})Cl_2]_2$ dimer (0.6 eq) and bipyridine ligand **5**, **6**, **7** or **8** (1 eq) in dry DMF (9 mL) was heated under MW irradiation at 70 ºC for 20–25 min. Then, a solution of 4,4'-dicarboxylic acid-2,2'-bipyridine (1.2 eq) in DMF (3 mL) was added, and the solution irradiated under MW at 135–150 ºC for additional 20 min. After cooling, a solution of NH_4SCN (25 eq) in DMF (3 mL), was added to the mixture, and irradiated again under MW at 135–150 ºC for 30–40 min. After cooling, DMF was removed from the flask by high-vacuum distillation. The remaining pasty solid was triturated in Et_2O (10mL), and the resulting suspension was filtered-off and then washed with Et_2O (2×10mL). The remaining solid was air-dried, dissolved in basic MeOH (NaOH) and purified by chromatography column on Sephadex™ (MeOH). The main band was collected, and the solvent evaporated to dryness, to afford the desired complex under the disodium salt form. This salt was redissolved in MeOH, and the resulting solution acidified by addition of a 10^{-2} M solution of HNO_3 in MeOH (0.5 eq of HNO_3 per eq of complex), affording the complex under the mono sodium salt form.

Dalton Transactions View Article Online DOI: 10.1039/C4DT01357C ARTICLE

Ru(II) complex TT206. According the general procedure, from [Ru(*p*-cymene)Cl_2]$_2$ (25.0 mg, 0.04 mmol), compound **6** (40.0 mg, 0.07 mmol), dcapy (20.0 mg, 0.08 mmol), and NH_4NCS, (131.0 mg, 1.73 mmol) to yield **TT206** (61 mg, 83%) as a dark-black reddish powder. ^{1}H NMR (300 MHz, [D6]DMSO, 25 ºC, TMS): δ = 9.45 (m, 2H), 9.18 (m, 1H), 9.09 (m, 1H), 8.94 (m, 1H), 8.32 (m, 1H), 8.19 (m, 2H), 8.02 (m, 2H), 7.92 (m, 1H), 7.63 (m, 2H), 7.42 (m, 1H), 7.33 (m, 2H), 1.52 (m, 4H), 1.43 (s, 12H), 1.30 (m, 4H), 1.21 (m, 4H), 0.88 ppm (m, 6H); UV-Vis (DMF): λ_{max}/nm (ε/M^{-1}·cm^{-1}) = 311 (35 600), 345 (sh., 24 200), 419 (sh., 12 100); MS (MALDI-TOF): *m/z* 984 [M-(NCS)]$^+$; HR-MS (MALDI-TOF): *m/z* calcd for $C_{45}H_{48}N_5O_4RuS_5$: 984.1353; found: 984.1361 [M-(NCS)]$^+$.

Ru(II) complex TT207. According the general procedure, from [Ru(*p*-cymene)Cl_2]$_2$ (20.0 mg, 0.03 mmol), compound **6** (40.0 mg, 0.05 mmol), dcapy (16.0 mg, 0.06 mmol), and NH_4NCS, (102.0 mg, 1.34 mmol) to yield **TT207** (37 mg, 56%) as a dark-black reddish powder. ^{1}H NMR (300 MHz, [D6]DMSO, 25 ºC, TMS): δ = 9.35 (m, 2H), 9.22 (m, 1H), 9.11 (m, 1H), 8.98 (m, 2H), 8.84 (m, 2H), 8.28 (m, 1H), 8.04 (m, 1H), 7.95 (m, 1H), 7.81 (m, 1H), 7.67 (m, 2H), 7.53 (m, 2H), 7.44 (m, 2H), 7.21 (m, 2H), 2.89 (m, 4H), 2.73 (s, 12H), 1.30 (m, 4H), 1.28 (m, 4H), 0.91 ppm (m, 6H); UV-Vis (DMF): λ_{max}/nm (ε/M^{-1}·cm^{-1})= 302 (39 900), 384 (33 800), 553 (15 300); MS (MALDI-TOF): *m/z* 1148 [M-(NCS)-Na+H)]$^+$, 1229 [M+H]$^+$; HRMS (MALDI-TOF): *m/z* calcd for $C_{54}H_{52}N_6O_4RuS_8$: 1206.0863[M-Na+H]$^+$; found: 1206.0820.

Ru(II) complex TT208. According the general procedure, from [Ru(*p*-cymene)Cl_2]$_2$ (22.0 mg, 0.04 mmol), compound **6** (40.0 mg, 0.06 mmol), dcapy (18.0 mg, 0.07 mmol), and NH_4NCS, (115.0 mg, 1.50 mmol) to yield **TT208** (56 mg, 82%) as a dark-black reddish powder. ^{1}H NMR (300 MHz, [D6]DMSO, 25 ºC, TMS): δ = 9.24 (m, 2H), 9.08 (m, 1H), 8.92 (m, 1H), 8.80 (m, 2H), 8.74 (m, 2H), 8.21 (m, 1H), 7.99 (m, 1H), 7.53 (m, 1H), 7.47 (m, 2H), 7.35 (m, 1H), 7.22 (m, 2H), 2.09 (m, 12H), 1.45 (m, 12H), 0.91 ppm (m, 18H); UV-Vis (DMF): λ_{max}/nm (ε/M^{-1}·cm^{-1})= 301 (43 800), 341 (30 200), 421 (12 200), 551 (13 100); MS (MALDI-TOF): *m/z* 1068 [M-(NCS)-Na+H]$^+$, 1149 [M+H]$^+$; HRMS (MALDI-TOF): *m/z* calcd for $C_{52}H_{60}N_6NaO_4RuS_6$: 1149.1946 [M+H]$^+$; found: 1149.1912 [M+H]$^+$.

Ru(II) complex TT209. According the general procedure, from [Ru(*p*-cymene)Cl_2]$_2$ (31.0 mg, 0.05 mmol), compound **6** (70.0 mg, 0.08 mmol), dcapy (24.0 mg, 0.10 mmol), and NH_4NCS, (160.0 mg, 2.10mmol) to yield **TT209** (53 mg, 48%) as a dark-black reddish powder. ^{1}H NMR (300 MHz, [D6]DMSO, 25 ºC, TMS): δ = 9.36 (m, 2H), 9.21 (m, 1H), 9.02 (m, 1H) 8.89 (m, 2H), 8.25 (m, 2H), 8.21(m, 1H), 8.03 (m, 1H), 7.95 (m, 1H), 7.84 (m, 1H), 7.63 (m, 2H), 7.52 (m, 2H), 7.41 (m, 2H), 7.11 (m, 2H), 1.39 (m, 12H), 0.89 ppm (m, 18H); UV-Vis (DMF): λ_{max}/nm (ε/M^{-1}·cm^{-1})= 300 (30 200), 385 (29 200), 552 (11 700); MS (MALDI-TOF): *m/z* 1232 [M-(NCS)-Na+H]$^+$, 1313 [M+H]$^+$; HRMS (MALDI-TOF): *m/z* calcd for $C_{59}H_{64}N_5O_4RuS_7$: 1232.2053 [M-(NCS)-Na+H]$^+$; found: 1232.2067.

(c) Device fabrication

The NSG10 (purchased from Nippon Sheet Glass company, Japan) FTO glass was washed in water and ethanol followed by 30 min ultrasonic cleaning in Deconnex™ solution. The TCO was then thermally treated at 520°C for 30 min to remove organic contaminants on the surface. The cleaned substrate was chemically treated in a 40 mM aqueous $TiCl_4$ solution for 30 min at 75°C, to form a TiO_2 underlayer. After this step, the nano crystalline TiO_2 (30 NRDT, Dyesol) films were prepared by screen printing technique followed by a series of sintering steps (325 °C for 5 min with 15 min ramp time, 375 °C for 5 min with 5 min ramp time, 450 °C for 15 min with 5 min ramp time, and 500 °C for 15 min with 5 min ramp time). Another $TiCl_4$ treatment was done following the procedure similar to the underlayer preparation. The films were further heated at 500°C for 30 min to remove the surface contaminants before dipping them in the dye solution. The sensitization was carried out for 14 hours at 25°C in dark and washed in acetonitrile to remove the loosely bound dye molecules before the cell assembly. For counter electrode, Pt coated TEC7 FTO (purchased from Solaronix, Switzerland) was used, and the Pt deposition was achieved by thermal decomposition at 410 °C for 20 min of a 2mM H_2PtCl_6 ethanolic solution drop casted on the FTO glass. The two electrodes were melt sealed using a 25 μm thick surlyn™ polymer film. Two different electrolytes were used in this study, coded as Z960 and Z984. Composition of electrolytes: i) for Z960: 1,2-dimethyl-3-propyl-imidazoliumiodide (DMII) [1 M], LiI [50 mM] , I_2 [30 mM], guanidinium thiocyanate (GuNCS) [0.1 M], and 4-*tert*-butylpyridine (TBP) [0.5 M], in a mixture of acetonitrile and valeronitrile (85:15, v/v); ii) for Z984: DMII [0.6 M], LiI [50 mM], I_2 [30 mM], GuNCS [0.1 M], and TBP [0.5 M], in a mixture of acetonitrile and valeronitrile (85:15, v/v). The electrolyte was injected by vacuum back filling technique through a hole sand blasted at the side of the counter electrode.

(d) Photovoltaic characterization procedures

The photovoltaic measurements were carried out with a 450 W xenon light source (Osram XBO 450, Germany) with a filter (Schott 113), whose power was regulated to the AM1.5G solar standard by using a reference Si photodiode equipped with a colour matched filter (KG-3, Schott) in order to reduce the mismatch in the region of 350–750 nm between the simulated light and AM1.5G to less than 4%. The devices were measured with a mask of area 0.159 cm^2. The applied potential and cell current were measured with a Keithley™ 2400 digital source meter. The incident photon-to-current conversion efficiency (IPCE) measurement was plotted as a function of wavelength by using the light from a 300 W xenon lamp (ILC Technology, USA), which was focused through a Gemini-180 double monochromator (Jobin Yvon Ltd., UK) onto the photovoltaic cell under testing. A computer controlled monochromator was incremented through the spectral range (300–900 nm) to generate a photocurrent action spectrum with a sampling

View Article Online
DOI: 10.1039/C4DT01357C

interval of 10 nm and a current sampling time of 4 s. In addition, photocurrent and continuous irradiated light intensity were measured simultaneously at each wavelength.

3. Results and discussion

(a) Synthesis

The synthesis of Ru(II)-dyes **TT206–209** is depicted in scheme 1. The first step involved an S-alkylation of 2-thiophenethiol with either 2-methyl-2-hexanol or 4-propyl-4-heptanol under BF_3-catalysed acidic conditions to afford compounds **1** and **2**, respectively. The corresponding stannyl derivatives of **1** and **2** were prepared by a one-pot reaction involving regioselective lithiatation/deprotonation at the α-position of thiophene derivatives with *n*BuLi in THF at low temperature, followed by subsequent reaction with $SnBu_3Cl$. Next, Pd-catalysed Stille cross-coupling with 2-bromothiophene in refluxing DMF afforded the upper generation, dithiophene compounds **3** and **4**.

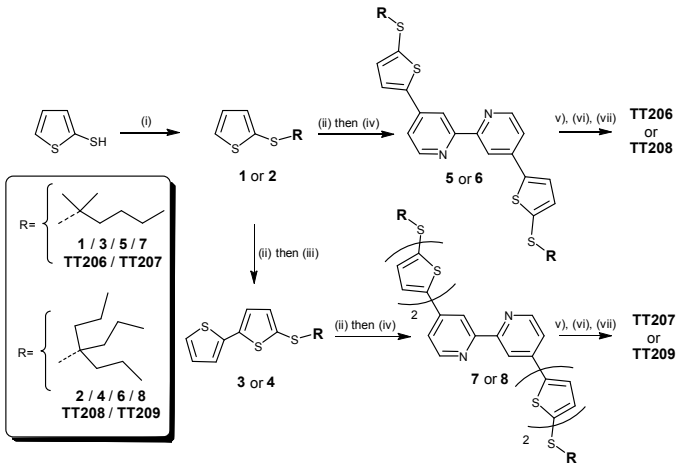

Scheme 1.Synthesis of bipyridine ligands **5-8** and Ru(II) complexes **TT206–TT209**. Reagent and conditions:(i) $BF_3{\cdot}OEt_2$, CH_2Cl_2,2-methyl-2-hexanol (for **1**) or 4-propyl-4-heptanol (for **2**),-10 ºC, 2h(**1**: 62%,**2**: 55%);(ii) *n*-butyllithium, THF, -78 ºC (30 min) to RT (1.5h) then $SnBu_3Cl$, THF, -78 ºC (30 min) to RT overnight (quantitative); (iii) 2-bromothiophene, DMF reflux, 24h (**3**: 52%, **4**: 65%);(iv) 4,4'-dibromo-2,2'-bipyridine, $Pd(PPh_3)_4$, DMF reflux, 48h (**5**: 54%; **6**: 53%, **7**: 47%, **8**: 48%) (v) $[Ru(p\text{-cymene})Cl_2]_2$, MW, 70 ºC, 20–25 min, followed by (vi) 4,4'-dicarboxylic acid-2,2'-bipyridine, DMF, MW 135–150 ºC, 20 min, and (vii) NH_4NCS, DMF, MW 135–150 ºC, 30–40 min (**TT206**: 83%, **TT207**: 56%, **TT208**: 82%, **TT209**: 48%).

By following the same reaction sequence than for **1** and **2**, the corresponding stannyl derivatives of **3** and **4** were obtained by treatment with *n*BuLi followed by reaction with $SnBu_3Cl$. The stannyl derivatives of **1**–**4** were then subjected to a Pd-catalysed Stille cross-coupling with 4,4-dibromo-2,2'-bipyridine in refluxing DMF to afford the corresponding functionalized bipyridine ligands **5**–**8**. Finally, the Ru(II) complexes **TT206**–**209** were prepared in a one-pot, three-step reaction under microwave-assisted standard procedures previously reported in the literature.[37] All compounds were characterized by NMR and UV-Vis spectroscopy, MS and HRMS spectrometry (copy of spectra are provided in the Supporting Information).

(b) UV-Vis absorption spectra

The UV-Vis spectra of the four dyes **TT206–209** in DMF solutions are depicted in Figure 1, and absorption data summarized in Table 1. Three- to four- distinct bands at around 300–310 nm, 340–450 nm and 550 nm can be observed for all complexes. For **TT206**/**208**, two distinct bands can be seen in the UV region: the first one at around 300–310 nm was assigned to ligand-centered charge-transfer (LCCT) transitions (π-π*) of the bipyridine moieties, and the second one at around 340 nm to the intraligand charge-transfer (ILCT) transition (π-π*) of the ancillary ligand; the two others absorption bands of lower energies in the visible region at around 420 and 550 nm, were ascribed to the metal-to-ligand charge-transfer (MLCT) transitions (4d-π*), characteristic of ruthenium(II) polypyridyl complexes. In the case of **TT207** and **TT209**, the broad and intense absorption band centred at around 400 nm, should contain the overlap of two components: the ILCT transition with major contribution, and the first MLCT transition (MLCT(1)) with minor contribution. The increase of both the electron donating ability and π-extended conjugation over the bipyridyl ancillary ligand from thiophene (**TT206** and **TT208**) to dithiophene groups (**TT207** and **TT209**) can be seen over this second absorption band: this antenna effect produced significant redshift and broadening, accompanied by stronger molar extinction coefficient for the formers. Regarding the lowest energy transition band (MLCT(2)), no significant variations were observed in the two series, and are in the range of values previously reported for the benchmarks **C106** and **CYCB11** dyes (MLCT(2) at 550 nm and 554 nm, respectively). Exception made of **TT206** that did not display a very well-defined maximum (quite broad) for the MLCT(2) band, all other dyes display redshift of 16–18 nm of this band in comparison with the homoleptic dye **N719**,[38] as expected for such heteroleptic Ru(II)-polypyridyl complex.

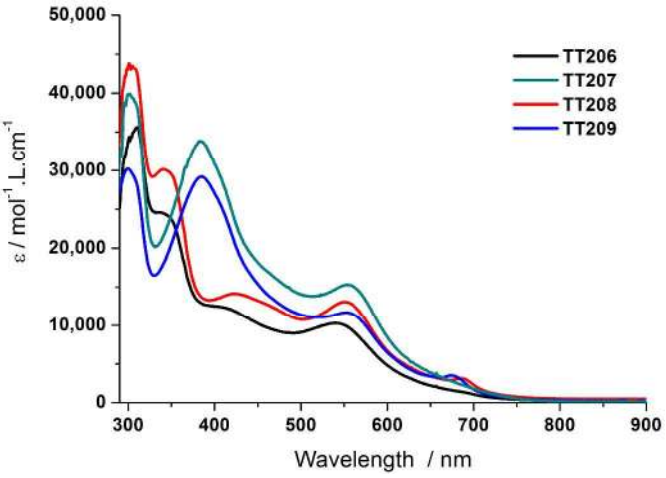

Figure 1. UV-Vis spectra of dyes **TT206–209** in DMF solution (the small blip at ~680 nm is due to an artefact of the apparatus)

Dalton Transactions View Article Online DOI: 10.1039/C4DT01357C ARTICLE

Table 1. UV-Vis absorption data of **TT** dyes, benchmarks **C106**,[35] **CYC-B11**[36] and **N719**[38] in DMF solution.

Dye	Transition band	λ_{max} (nm)	ε ($/10^4$ M^{-1} cm^{-1})[a]
TT206	LCCT	311	3.56
	ILCT	345	2.42
	MLCT(1)	~419(sh)	1.21
	MLCT(2)	~539(br)	1.03
TT207	LCCT	302	3.99
	ILCT[b]+MLCT(1)	384	3.38
	MLCT(2)	553	1.53
TT208	LCCT	301	4.38
	ILCT	341	3.02
	MLCT(1)	421	1.42
	MLCT(2)	551	1.31
TT209	LCCT	300	3.20
	ILCT[b]+MLCT(1)	385	2.92
	MLCT(2)	552	1.17
C106[c]	LCCT	310	*(n.a.)*
	ILCT[b]+MLCT(1)	348 (br)	*(n.a.)*
	MLCT(2)	550	1.87
CYCB11[c]	LCCT	305	*(n.a.)*
	ILCT[b]+MLCT1	388	*(n.a.)*
	MLCT2	554	2.42
N719[c]	LCCT	312	4.91
	MLCT1	396	1.43
	MLCT2	535	1.47

[a]ε values of **TT** dyes are given within a margin of error of ±10%. [b]Main contribution is coming from the ILCT transition. [c]Values collected from the literature; see refs [35], [36] and [38].

(LCCT= Ligand-Centered Charge-Transfer; ILCT= Intraligand Charge-Transfer; MLCT= Metal-to-Ligand Charge-Transfer)

(c) Photovoltaic performances

The photovoltaic performances of the TT-sensitized DSSCs were tested under simulated AM1.5G Illumination (power 100 mW cm^{-2}), using our standard electrolyte (Z960) containing the iodine/triiodine couple as redox shuttle. These data are summarized in Table 2. Figure 2 depicts the IPCE action spectra for each DSSC. The IPCE values reached 40–80% in the 400–700 nm region for the four cells, with maximum values at around ~550 nm, which correspond to the maximum of absorption of the second MLCT band.

Table 2. Photovoltaic parameters of DSSC devices made with **TT206-209** sensitizers measured under AM1.5G solar irradiance (100 mW/cm^2).

Dye	Analogues Series	Chain type[a]	J_{SC} (mA/cm^2)	V_{OC} (mV)	F.F. (%)	η (%)
TT206	C106	I	15.9	632.5	75.0	7.5
TT207	B11	I	17.2	666.5	73.9	8.5
TT208	C106	II	12.7	629.0	76.8	6.1
TT209	B11	II	16.5	668.9	72.0	8.0

[a]Type I = 2-methylhex-2-yl; Type II = 1,1-dipropylbutyl

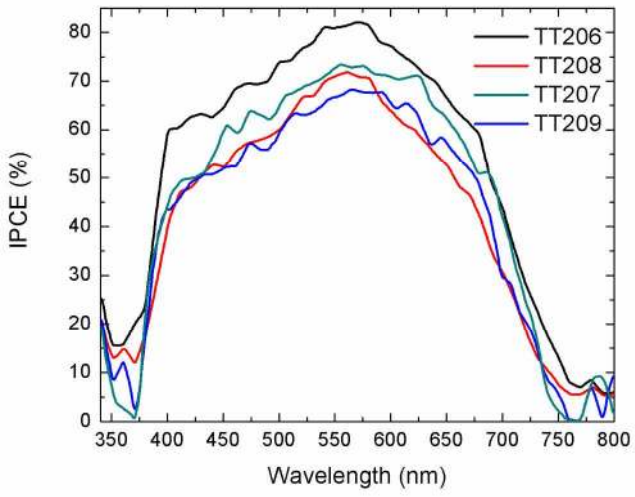

Figure 2. IPCE action spectra of DSSC devices made with **TT206-209** dyes.

Because of dye-aggregation issues, the IPCE values did not match perfectly with their relative short circuit current densities values (J_{SC}). The type of substitution, 2-methylhex-2-yl (Type I) or 1,1-dipropylbutyl (Type II), follows the same trends in each series. First, the open-circuit voltage (V_{OC}) is almost unchanged regardless to the type of substitution: V_{OC}= 632.5 mV and 629 mV, for **TT206** and **TT208** (**C106** analogues), respectively, and V_{OC}= 666.5 mV and 668.9 mV, for **TT207** and **TT209** (**CYC-B11** analogues), respectively. The main difference is coming from much larger J_{SC} for type I than for type II, which mostly account for their superior overall PCE. Now, if we compare dyes with the same type of substitution, same trends can be observed: lower fill factor for **CYC-B11** analogues than for **C106** ones, but which is overcompensated by larger V_{OC} and J_{SC}, and accordingly it results in higher PCE. The extension and redshift of absorption in **CYC-B11** analogues caused by the presence of the dithiophene moieties must confer to these dyes a better light-harvesting efficiency in comparison with their **C106** analogues, which explain well the larger J_{SC} of these cells. Moreover, the significantly greater V_{OC} achieved by **CYC-B11** analogues than **C106** ones (ΔV_{OC}= +34–40 mV), suggests reduced recombination rates at the TiO_2 / electrolyte interface between oxidized I_3^- ions and injected electrons. We assume that the bulky groups located at farther distances from the TiO_2 surface in **CYC-B11** analogues should act as a more efficient blocking layer than in **C106** ones to prevent the penetration of oxidized species to the TiO_2 surface. The best performing dye of the series, **TT207**, was further optimized with respect to dye-uptake solvent and electrolyte composition (Table 3). The highest PCE of DSSC devices made with **TT207** dye was obtained when using γ-butyrolactone (GBL) as dye-uptake solvent and Z984 as electrolyte. In comparison with our standard conditions (DMF/Z960), the fill factor was slightly decreased, but overcompensated by increases of both J_{SC} and V_{OC}, thus resulting in an improved overall PCE of 9.1%.

View Article Online
DOI: 10.1039/C4DT01357C

Table 3. Optimization of **TT207** DSSCs with respect to dye-uptake solvent and electrolyte (photovoltaic parameters of devices measured under AM1.5G solar irradiance (100 mW/cm^2)).

Dye-uptake Solvent	Electrolyte[a]	J_{SC} (mA/cm^2)	V_{OC} (mV)	F.F. (%)	η (%)
DMF	Z960	17.2	666.5	73.9	8.5
GBL	Z960 +50mM NaI	18.5	668.7	70.5	8.9
EtOH	Z984	18.5	682.3	70.4	8.9
MeOH	Z984	18.6	661.9	70.6	8.7
GBL	Z984	18.7	683.1	71.6	9.1
AcCN/*t*-BuOH (1:1, v/v) +10% GBL	Z984	17.0	665.0	72.8	8.2

[a] See details of the electrolyte compositions in the experimental section (GBL = γ-butyrolactone)

Conclusion

The photovoltaic performances of four novel ruthenium dyes **TT206-209**, analogues of **C106** or **CYC-B11** sensitizers, have been tested in DSSC. Two types of branched alkyl chains, either 2-methylhex-2-yl (Type I) or 1,1-dipropylbutyl (Type II), have been used to design these dyes, and their performances in DSSC compared in both series. The 2-methylhex-2-yl substitution pattern was found more efficient in both **C106** and **CYC-B11** series, which provide some guidelines to design Ru-(II)bipyridine dyes for DSSCs. The dye **TT207** that posses extended and redshifted absorption caused by dithiophene moieties in the ancillary group (**CYC-B11** analogue), and 2-methylhex-2-yl type substitution (Type I), logically achieved the highest PCE of the series (η= 8.5%). Further optimization of **TT207**/DSSCs, with respect to the dye-uptake solvent and electrolyte composition, led to a PCE of 9.1% under AM1.5G standard conditions.

Acknowledgements

Financial support is acknowledged from European Union within the FP7-ENERGY-2012-1 framework, GLOBALSOL project, Proposal No 309194-2 and the Spanish MEC and MICINN (CTQ2011-24187/BQU and PRI-PIBUS-2011-1128). MKN thank the Center of Excellence for Advanced Materials Research (CEAMR), King Abdulaziz University, Jeddah, Saudi Arabia for distinguished Adjunct Professor program.

Notes and references

1 M. Grätzel, *Acc. Chem. Res.*, 2009, **42**, 1788-1798.
2 T. Bessho, S. M. Zakeeruddin, C.-Y.Yeh, E. W.-G. Diau and M. Grätzel, *Angew. Chem., Int. Ed.*, 2010, **49**, 6646-6649.
3 A. Yella, H.-W. Lee, H. N. Tsao, C. Yi, A. K. Chandiran, M. K. Nazeeruddin, E. W.-G. Diau, C.-Y.Yeh, S. M. Zakeeruddin and M. Grätzel, *Science*, 2011, **334**, 629-634.
4 S. Mathew, A. Yella, P. Gao, R. Humphry-Baker, F. E. CurchodBasile, N. Ashari-Astani, I. Tavernelli, U. Rothlisberger, M. K. Nazeeruddin and M. Grätzel, *Nat. Chem.*, 2014, **6**, 242-247.
5 A. Yella, C.-L.Mai, S. M. Zakeeruddin, S.-N.Chang, C.-H.Hsieh, C.-Y.Yeh and M. Grätzel, *Angew. Chem., Int. Ed.*, 2014, **53**, 2973-2977.
6 S. Ardo and G. J. Meyer, *Chem. Soc. Rev.*, 2009, **38**, 115-164.
7 J.-F. Yin, M. Velayudham, D. Bhattacharya, H.-C.Lin and K.-L. Lu, *Coord. Chem. Rev.*, 2012, **256**, 3008-3035.
8 A. Abbotto and N. Manfredi, *Dalt. Trans.*, 2011, **40**, 12421-12438.
9 P. G. Bomben, T. J. Gordon, E. Schott and C. P. Berlinguette, *Angew. Chem., Int. Ed.*, 2011, **50**, 10682-10685.
10 J. Xu, H. Wu, X. Jia and D. Zou, *Chem. Comm.*, 2012, **48**, 7793-7795.
11 J. J. Lagref, M. K. Nazeeruddin and M. Grätzel, *Synth. Met.*, 2003, **138**, 333-339.
12 C. Klein, M. K. Nazeeruddin, D. Di Censo, P. Liska and M. Grätzel, *Inorg. Chem.*, 2004, **43**, 4216-4226.
13 S. Lense, K. I. Hardcastle and C. E. MacBeth, *Dalton Trans.*, 2009, 7396-7401.
14 C.-Y. Chen, S.-J.Wu, C.-G.Wu, J.-G.Chen and K.-C. Ho, *Angew. Chem., Int. Ed.*, 2006, **45**, 5822-5825.
15 A. Mishra, N. Pootrakulchote, M. K. R. Fischer, C. Klein, M. K. Nazeeruddin, S. M. Zakeeruddin, P. Bauerle and M. Gratzel, *Chem. Comm.*, 2009, 7146-7148.
16 S.-J. Wu, C.-Y.Chen, J.-G.Chen, J.-Y.Li, Y.-L.Tung, K.-C.Ho and C.-G. Wu, *Dyes Pigm.*, 2010, **84**, 95-101.
17 C. Y. Chen, H. C. Lu, C. G. Wu, J. G. Chen and K. C. Ho, *Adv. Funct. Mater.*, 2007, **17**, 29-36.
18 F. Gao, Y. Wang, D. Shi, J. Zhang, M. Wang, X. Jing, R. Humphry-Baker, P. Wang, S. M. Zakeeruddin and M. Grätzel, *J. Am. Chem. Soc.*, 2008, **130**, 10720-10728.
19 A. Abbotto, C. Barolo, L. Bellotto, F. D. Angelis, M. Grätzel, N. Manfredi, C. Marinzi, S. Fantacci, J.-H. Yum and M. K. Nazeeruddin, *Chem. Comm.*, 2008, 5318-5320.
20 D. Shi, N. Pootrakulchote, R. Li, J. Guo, Y. Wang, S. M. Zakeeruddin, M. Grätzel and P. Wang, *J. Phys. Chem. C*, 2008, **112**, 17046-17050.
21 M. Chandrasekharam, T. Suresh, S. P. Singh, B. Priyanka, K. Bhanuprakash, A. Islam, L. Han and M. Lakshmi Kantam, *Dalton Trans.*, 2012, **41**, 8770-8772.
22 L. Giribabu, C. Vijay Kumar, C. S. Rao, V. G. Reddy, P. Y. Reddy, M. Chandrasekharam and Y. Soujanya, *Energy Environ. Sci.*, 2009, **2**, 770-773.
23 F. Matar, T. H. Ghaddar, K. Walley, T. DosSantos, J. R. Durrant and B. O'Regan, *J. Mat. Chem.*, 2008, **18**, 4246-4253.
24 D. Kuang, S. Ito, B. Wenger, C. Klein, J.-E. Moser, R. Humphry-Baker, S. M. Zakeeruddin and M. Grätzel, *J. Am. Chem. Soc.*, 2006, **128**, 4146-4154.
25 S.-R. Jang, C. Lee, H. Choi, J. J. Ko, J. Lee, R. Vittal and K.-J. Kim, *Chem. Mat.*, 2006, **18**, 5604-5608.
26 C.-Y. Chen, N. Pootrakulchote, S.-J.Wu, M. Wang, J.-Y.Li, J.-H.Tsai, C.-G. Wu, S. M. Zakeeruddin and M. Grätzel, *J. Phys. Chem. C*, 2009, **113**, 20752-20757.
27 S. A. Haque, S. Handa, K. Peter, E. Palomares, M. Thelakkat and J. R. Durrant, *Angew. Chem., Int. Ed.*, 2005, **44**, 5740-5744.
28 H. J. Snaith, C. S. Karthikeyan, A. Petrozza, J. l. Teuscher, J. E. Moser, M. K. Nazeeruddin, M. Thelakkat and M. Grätzel, *J. Phys. Chem. C*, 2008, **112**, 7562-7566.

Dalton Transactions

View Article Online
DOI: 10.1039/C4DT01357C ARTICLE

29 N. Hirata, J.-J.Lagref, E. J. Palomares, J. R. Durrant, M. K. Nazeeruddin, M. Grätzel and D. Di Censo, *Chem. Eur. J.*, 2004, **10**, 595-602.

30 S.-W. Wang, K.-L. Wu, E. Ghadiri, M. G. Lobello, S.-T. Ho, Y. Chi, J.-E. Moser, F. De Angelis, M. Grätzel and M. K. Nazeeruddin, *Chem. Sci.*, 2013, **4**, 2423-2433.

31 K.-L. Wu, W.-P. Ku, J. N. Clifford, E. Palomares, S.-T. Ho, Y. Chi, S.-H. Liu, P.-T. Chou, M. K. Nazeeruddin and M. Grätzel, *Energy Environ. Sci.*, 2013, **6**, 859-870.

32 T. Funaki, H. Kusama, N. Onozawa-Komatsuzaki, K. Kasuga, K. Sayama and H. Sugihara, *Eur. J. Inorg. Chem.*, 2014, **2014**, 1303-1311.

33 M. Garcia-Iglesias, L. Pelleja, J.-H. Yum, D. Gonzalez-Rodriguez, M. K. Nazeeruddin, M. Grätzel, J. N. Clifford, E. Palomares, P. Vazquez and T. Torres, *Chem. Sci.*, 2011, **3**, 1177-1184.

34 J. N. Clifford, E. Martinez-Ferrero, A. Viterisi and E. Palomares, *Chem. Soc. Rev.*, 2011, **40**, 1635-1646.

35 Y. Cao, Y. Bai, Q. Yu, Y. Cheng, S. Liu, D. Shi, F. Gao and P. Wang, *J. Phys. Chem. C*, 2009, **113**, 6290-6297.

36 C.-Y. Chen, M. Wang, J.-Y.Li, N. Pootrakulchote, L. Alibabaei, C.-h.Ngoc-le, J.-D.Decoppet, J.-H.Tsai, C. Grätzel, C.-G. Wu, S. M. Zakeeruddin and M. Grätzel, *ACS Nano*, 2009, **3**, 3103-3109.

37 K. Willinger, K. Fischer, R. Kisselev and M. Thelakkat, *J. Mat. Chem.*, 2009, **19**, 5364-5376.

38 N. Hirata, J.-J. Lagref, E. J. Palomares, J. R. Durrant, M. K. Nazeeruddin, M. Grätzeland D. Di Censo, *Chem. Eur. J.*, 2004, **10**, 595-602.

View Article Online
DOI: 10.1039/C4DT01357C

Dalton Transactions

RSCPublishing

Table of Contents Entry

Branched and Bulky Substituted Ruthenium Sensitizers for Dye-Sensitized Solar Cells

M. Sánchez Carballo,[a] M. Urbani,[a,b] A. Kumar Chandiran,[c] D. González-Rodríguez,[a] P. Vázquez,[a] M. Grätzel,[c] M.K. Nazeeruddin*[c] and T. Torres*[a,b]

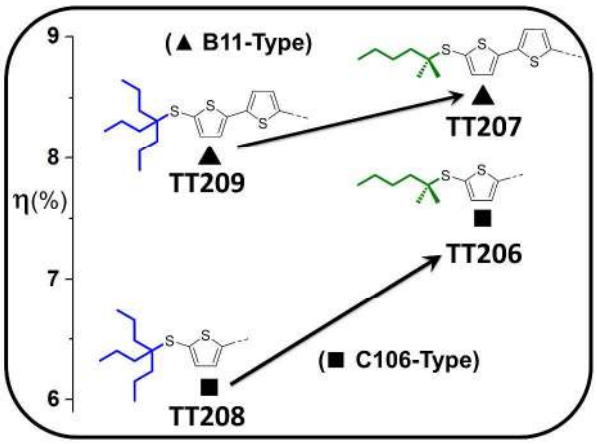

Four novel Ru(II)-sensitizers (**TT206–209**) incorporating two different types of branched and bulky alkyl chains, were tested in TiO_2-DSSCs.

Abstract: We report on the synthesis, and photovoltaic performances of four novel Ru(II)-bipyridine heteroleptic complexes **TT206–209**, incorporating branched and bulkier alkyl chains compared to their linear analogues **C106** and **CYC-B11** previously reported. In both series, we found that dyes containing 2-methyl-hex-2-yl substitution gave better performances than 1,1-dipropylbutyl. The best overall performances over the four dyes were obtained for **TT207** (**CYC-B11** analogue) that contain 2-methylhex-2-yl type substitution, achieving an overall PCE of 8.5%. Further optimization of **TT207**/DSSCs, with respect to the dye-uptake solvent and electrolyte composition, led to a maximum PCE of 9.1% under AM1.5G standard conditions.

View Article Online
DOI: 10.1039/C4DT01357C

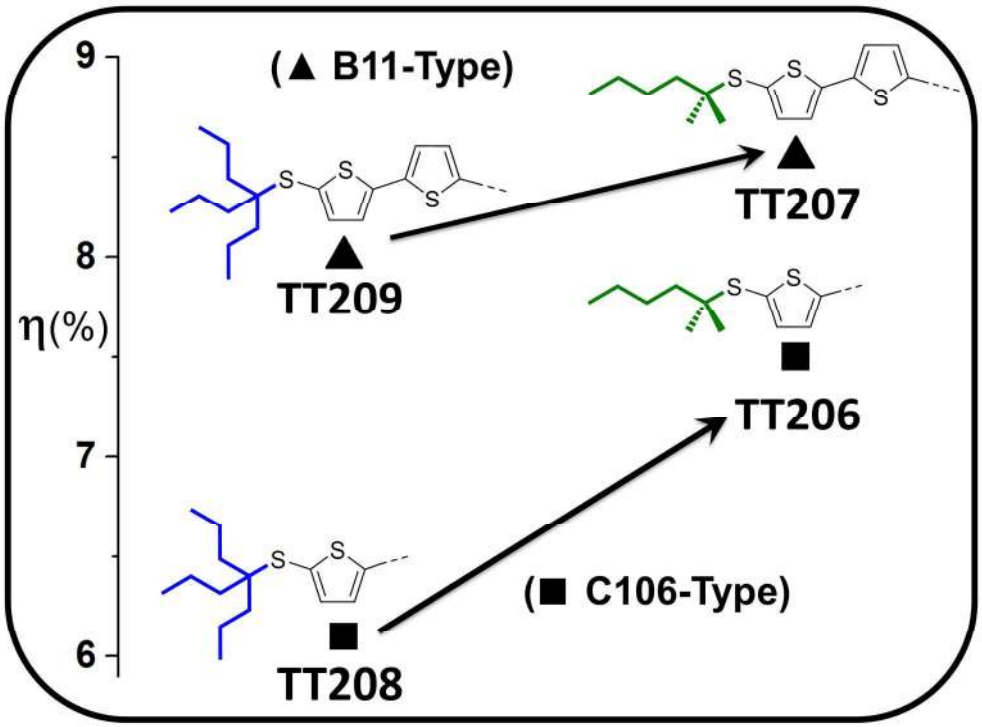

190x142mm (300 x 300 DPI)